

Ref. 3.)

In closing, we note that the important role played by the recombination phonons stems from the fact that they are generated at a great rate, i.e., of order I_0 , and that β is relatively large and comparable with τ_γ^{-1} . As a result, the phonons produced by the recombination of the injected quasiparticles will themselves create quasiparticles at a rate comparable with I_0 . On the other hand, it may be possible to minimize the effects of the phonons by carrying out a pulse experiment. For times small compared with τ_R , the number of recombination phonons will be negligible and thus the initial decay rate of a pulse of injected quasiparticles will be determined solely by τ_R .

We should like to thank M. A. Lampert for an illuminating discussion, and B. I. Miller and A. H. Dayem for helpful discussions and a preprint of their paper prior to publication.

¹D. M. Ginsberg, Phys. Rev. Letters 8, 204 (1962). See also Discussion 33, Rev. Mod. Phys. 36, 215 (1964).

²B. N. Taylor, thesis, University of Pennsylvania,

1963.

³B. I. Miller and A. H. Dayem, Bull. Am. Phys. Soc. 12, 310 (1967); Phys. Rev. Letters 18, 1000 (1967).

⁴This recombination takes place primarily via phonon emission rather than photon emission. See E. Burstein, D. H. Langenberg, and B. N. Taylor, Phys. Rev. Letters 6, 92 (1961), and also Refs. 6-8.

⁵J. R. Schrieffer and D. M. Ginsberg, Phys. Rev. Letters 8, 207 (1962).

⁶A. Rothwarf and M. Cohen, Phys. Rev. 130, 1401 (1963).

⁷G. Lucas and M. J. Stephen, Phys. Rev. 154, 349 (1967).

⁸This was calculated using the Umklapp process rate for Al as done for Pb in Ref. 6.

⁹It is assumed that the quasiparticles are injected at the gap edge and that the energy of the recombination phonons is 2Δ where Δ is the energy gap parameter.

¹⁰C. Kittel, *Introduction to Solid State Physics* (John Wiley & Sons, New York, 1957), 2nd ed., p. 366.

¹¹Other decay modes such as electron-phonon and phonon-phonon scattering must have a lifetime longer than 8.5×10^{-12} sec since even at room temperature, such lifetimes are longer than this (see Ref. 10, p. 149).

¹²It is unlikely that any temperature dependence in τ_γ would be sufficiently strong to invalidate these conclusions.

EFFECT OF BOUND STATES ON THE EXCITATION SPECTRUM OF A HEISENBERG FERROMAGNET AT LOW TEMPERATURE*

Richard Silberglitt† and A. Brooks Harris

Department of Physics, University of Pennsylvania, Philadelphia, Pennsylvania
(Received 22 May 1967)

A compact expression for the energy shift and inverse lifetime (energy width) of spin waves in a Heisenberg ferromagnet at low temperatures is given. The two-particle bound states are observable via the resonance they cause in the self-energy of spin waves.

The purpose of this brief note is to report calculations of the transverse component of the generalized wave-vector and frequency-dependent susceptibility $\chi_{+-}(k, \omega)$ for the Heisenberg ferromagnet at low temperatures. These calculations show that at short wavelengths the two-particle bound states¹ influence the single-particle spin-wave excitations in a dominant and nonperturbative way.

We use the Dyson-Maleev transformation²

$$\begin{aligned} S_+ &= (2S)^{1/2}(1 - a^\dagger a / 2S)a; & S_- &= (2S)^{1/2}a^\dagger; \\ S_z &= S - a^\dagger a \end{aligned} \quad (1)$$

to write the Heisenberg Hamiltonian in terms of boson operators as

$$\begin{aligned} H = E_0 + \sum_k \epsilon_k a_k^\dagger a_k + \frac{1}{2N} \sum_{k\lambda\lambda'} V_k(\lambda, \lambda') \\ \times a_{\frac{1}{2}k+\lambda}^\dagger a_{\frac{1}{2}k-\lambda}^\dagger a_{\frac{1}{2}k+\lambda} a_{\frac{1}{2}k-\lambda}, \end{aligned} \quad (2)$$

where

$$\epsilon_k = J_z S(1 - \gamma_k), \quad (3a)$$

$$V_k(\lambda, \lambda') = -\frac{1}{2}J_z [\gamma_{\lambda-\lambda'} + \gamma_{\lambda+\lambda'} - \gamma_{\frac{1}{2}k+\lambda} - \gamma_{\frac{1}{2}k-\lambda}] \quad (3b)$$

in the usual notation.³ The susceptibility is

the retarded Green's function $\langle\langle S_+; S_- \rangle\rangle$ or in the boson representation $2S\langle\langle [1 - a^\dagger a / 2S] a; a^\dagger \rangle\rangle$ and can be written as⁴

$$\chi_{+-}(k, \omega) = 2S[1 - (1/2S)\Lambda(k, \omega)]G(k, \omega), \quad (4)$$

where $\Lambda(k, \omega)$ is a vertex function and $G(k, \omega)$ is the single-particle boson Green's function which we write as $G(k, \omega) \equiv [\omega - \epsilon_k - \Sigma(k, \omega)]^{-1}$. The new analytic result we give here is a compact expression for the self-energy $\Sigma(k, \omega)$ for $\omega = \epsilon_k$ from which one obtains the temperature-dependent excitation energy,

$$\epsilon_k(T) = \epsilon_k + \Sigma'(k, \epsilon_k), \quad (5a)$$

and energy width,

$$\Delta\omega_k(T) = \Sigma''(k, \epsilon_k), \quad (5b)$$

of short-wavelength spin waves. Here $\Sigma'(k, \omega)$ and $\Sigma''(k, \omega)$ are the real and imaginary parts of $\Sigma(k, \omega)$. Although these two quantities are directly observable via the inelastic scattering of neutrons,⁵ no Heisenberg ferromagnet has yet been studied in the spin-wave region. However, with the recent availability of higher flux sources of neutrons and the concomitant gain in resolution, experimental determin-

ations of $\epsilon_k(T)$ and $\Delta\omega_k(T)$ to test our calculations can be anticipated. Calculations of the full frequency dependence of $\chi_{+-}(k, \omega)$ have been carried out and will be reported elsewhere.

We evaluate $\Sigma(k, \omega)$ at low temperatures as the sum of contributions from all diagrams involving a single boson hole (i.e., backward) line. This sum is conveniently expressed in terms of the t matrix, which is the sum of all ladder diagrams with no hole lines, since a hole line will be needed to close two free ends of the ladder to obtain a diagram for $\Sigma(k, \omega)$ (see Fig. 1). For $kT \ll \epsilon_k$ one has

$$\Sigma(k, \omega) = \frac{2}{N} \sum_p t(\omega + \epsilon_p; k + p; \frac{1}{2}(k-p), \frac{1}{2}(k-p)) n_p. \quad (6)$$

To evaluate (6) we need the t matrix at zero temperature, which is the solution to

$$t(z; k; \lambda, \mu) = V_k(\lambda, \mu) + \frac{1}{N} \sum_\rho V_k(\lambda, \rho) \frac{t(z; k; \rho, \mu)}{z - \epsilon_{\frac{1}{2}k + \rho} - \epsilon_{\frac{1}{2}k - \rho}}. \quad (7)$$

This equation is similar to that solved by Wor-tis¹ and has the solution

$$t(z; k; \lambda, \mu) = 2J \sum_{i,j=x,y,z} (\cos \frac{1}{2}k_i - \cos \mu_i) \left[\left(1 - \frac{1}{2S} B(k, z) \right)^{-1} \right]_{ij} \cos \lambda_j, \quad (8)$$

where $\mathbf{1}$ is the unit tensor and where $B_{ij}(k, z)$ is defined in Ref. 1. Substituting this expression into (6), we find, to lowest order in $\tau = kT/J_S$,

$$\Sigma(k, \omega) = \Sigma^{(1)}(k) \left\{ \frac{2}{3} \sum_{i=x,y,z} \left[\left(1 - \frac{1}{2S} B(k, \omega) \right)^{-1} \right]_{ii} \frac{\sin^2 \frac{1}{2}k_i}{1 - \gamma_k} + \frac{4}{3} \sum_{i,j=x,y,z} \frac{\sin \frac{1}{2}k_i \cos \frac{1}{2}k_j}{1 - \gamma_k} \frac{\partial}{\partial k_i} \left[\left(1 - \frac{1}{2S} B(k, \omega) \right)^{-1} \right]_{ij} \right\}, \quad (9)$$

where $\Sigma^{(1)}(k)$ is the first Born approximation for $\Sigma(k, \omega)$:

$$\Sigma^{(1)}(k) = -(\epsilon_k/32S)\pi^{-3/2} \zeta(\frac{5}{2}) \tau^{5/2}. \quad (10)$$

When $\omega = \epsilon_k$ and k lies along the (111) direction, the sum rules¹ on $B_{ij}(k, \omega)$ and its derivatives lead to simplifications. Then we write

$$\Sigma(k, \epsilon_k) = \Sigma^{(1)}(k) Q(k), \quad (11a)$$

$$Q(k) = 1 + \frac{4\Gamma(k)}{3[2S - \Gamma(k)]} + \frac{\alpha(k)}{3S}, \quad (11b)$$

where

$$\Gamma(k) = \frac{3}{N} \sum_\lambda \frac{(\cos \frac{1}{2}k - \cos \lambda_y) \cos \lambda_x}{D \cos \frac{1}{2}k}, \quad (12a)$$

$$\alpha(k) = \frac{3}{N} \sum_\lambda D^{-1} \cos \lambda_x, \quad (12b)$$

where

$$D \equiv 3 \cos \frac{1}{2}k - \sum_{i=x,y,z} \cos \lambda_i - i\epsilon. \quad (12c)$$

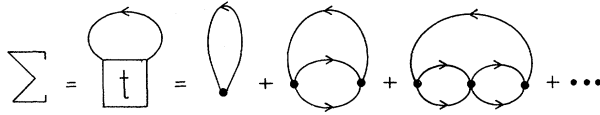


FIG. 1. Graphs which contribute to the self-energy $\Sigma(k, \omega)$ at low temperature. The box labeled t represents the sum of all ladder diagrams, i.e., the t matrix.

For $k \rightarrow 0$, $\text{Re}Q(k)$ reduces to Dyson's expression.⁶ Numerical evaluation of $\Sigma'(k, \epsilon_k)$ and $\Sigma''(k, \epsilon_k)$ are plotted for spin $\frac{1}{2}$ in Fig. 2.

Several features of these results are noteworthy. Firstly, one sees the resonancelike behavior of $\Sigma(k, \epsilon_k)$ due to the factor $1 - \Gamma(k)$ as $\text{Re}\Gamma(k)$ approaches unity near⁷ $k = 124^\circ$. This is a manifestation of one of the two-particle bound states which (although somewhat damped) persists into the two-particle continuum⁸ and whose energy coincides with the spin-wave energy

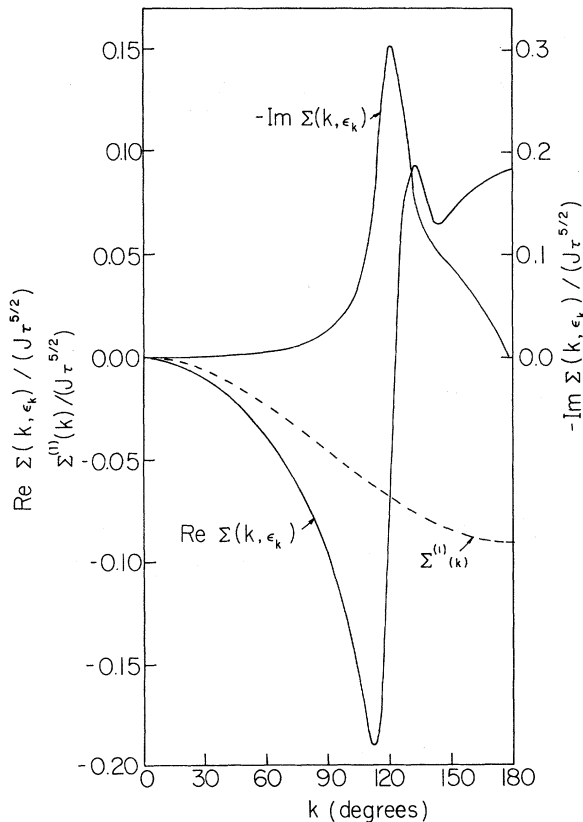


FIG. 2. Real and imaginary parts of the self-energy $\Sigma(k, \epsilon_k)$ for spin $\frac{1}{2}$ and k lying along the [111] direction (Ref. 7), as given by Eq. (11). The dashed curve is $\Sigma^{(1)}(k)$, the first Born approximation to $\Sigma(k, \epsilon_k)$. The energy of the two-particle scattering resonance coincides with the spin-wave energy at $k = 124^\circ$.

at $k = 124^\circ$. Secondly, one sees that $Q(k) \sim 1$ only at long wavelength, from which we conclude that the first Born approximation is only reasonable in that regime. For short wavelengths the Born approximation is completely misleading. As the spin value is increased, the first Born approximation remains reasonable to successively shorter wavelengths. Since perturbation theory corresponds to expansion of $[1 - \Gamma(k)]^{-1}$ in a geometric series, one sees that perturbation theory will converge only for $|\Gamma(k)| < 1$, that is for $k \leq 120^\circ$. Thirdly, for short wavelengths, the energy renormalization changes sign, becoming positive. This unexpected result can be understood physically as the repulsion between the single-particle excitation and the bound states (analogous to the repulsion of energy levels in perturbation theory). We have verified these results by explicit numerical checks of the sum rules on $\chi_{+-}(k, \omega)$. The average energy $\langle \omega \rangle$ is defined to be

$$\langle \omega \rangle = \frac{\int_{-\infty}^{+\infty} \omega' [\text{Im} \chi_{+-}(k, \omega')] d\omega'}{\int_{-\infty}^{+\infty} [\text{Im} \chi_{+-}(k, \omega')] d\omega'}, \quad (13a)$$

which can be written exactly as

$$\langle \omega \rangle = \frac{\langle [S_{k+}, [H, S_{k-}]] \rangle}{\langle [S_{k+}, S_{k-}] \rangle}. \quad (13b)$$

We have evaluated Eq. (13) rigorously to order $\tau^{5/2}$ and find

$$\langle \omega \rangle = \epsilon_k + \Sigma^{(1)}(k), \quad (14)$$

which is always less than ϵ_k , as expected. We find that the upwards renormalization of the spin-wave energy is compensated by the small amount of weight in $\text{Im} \chi_{+-}(k, \omega)$ at the bound states in just such a way that Eq. (14) obtains.

Finally, we should comment on the range of validity of our results. First of all, the energy shift is only given by $\Sigma'(k, \epsilon_k)$ when that function does not vary rapidly with ω . This will be true except very near the edge of the zone. Accordingly we estimate that $\Sigma'(k, \epsilon_k)$ can only be interpreted as the energy shift for $180^\circ - k \geq O(T^{5/2})$, which for $kT/JS = \frac{1}{2}$ gives $k \leq 178^\circ$. Also our calculations neglect processes involving the simultaneous interaction of three or more spin waves. Again such effects

are most serious near the edge of the zone. We expect that our results should be valid in the same temperature range as Dyson's, since both the thermodynamic quantities calculated by Dyson and the dynamical properties we calculate are influenced by long-wavelength thermal spin waves. On the other hand, one might argue that since the effects we find depend intimately on the influence of bound states, our results will be valid only in the (possibly smaller) temperature range where bound states are meaningful. However, it seems to us that these two regions are essentially the same, since when many spin-wave processes become important (and two-particle bound states lose their meaning), Dyson's formulas must also break down.

The authors wish to thank Dr. D. Hone for

helpful advice on the calculations of $B_{ij}(k, \omega)$.

*Work supported in part by the National Science Foundation under Grant No. GP 6771 and by the Advanced Research Projects Agency.

†National Aeronautics and Space Administration predoctoral fellow.

¹M. Wortis, Phys. Rev. **132**, 85 (1963).

²F. J. Dyson, Phys. Rev. **102**, 1217 (1956); S. V. Mal'eev, Zh. Eksperim. i Teor. Fiz. **33**, 1010 (1957) [translation: Soviet Phys.-JETP **6**, 776 (1958)].

³T. Oguchi, Phys. Rev. **117**, 117 (1960).

⁴S. V. Peletminskii and V. G. Bar'yakhtar, Fiz. Tverd. Tela **6**, 219 (1964) [translation: Soviet Phys.-Solid State **6**, 174 (1964)].

⁵K. C. Turberfield, A. Okazaki, and R. W. H. Stevenson, Proc. Phys. Soc. (London) **85**, 743 (1965).

⁶F. J. Dyson, Phys. Rev. **102**, 1230 (1956), Eq. (138).

⁷By $k = d^\circ$ we mean $ak_x = ak_y = ak_z = d\pi/180$.

⁸R. G. Boyd and J. Callaway, Phys. Rev. **138**, A1621 (1965).

STATIC QUADRUPOLE MOMENT OF THE FIRST 2^+ STATE IN ^{114}Cd MEASURED BY COULOMB EXCITATION*

J. E. Glenn and J. X. Saladin

University of Pittsburgh, Pittsburgh, Pennsylvania

(Received 22 May 1967)

Recently, several experiments¹⁻⁴ have been reported which make use of higher order effects in Coulomb excitation in order to determine quadrupole moments of excited states of nuclei. One of the surprising results of these measurements was the systematic occurrence of large quadrupole moments for the first 2^+ states of nuclei which heretofore were believed to be good examples of the harmonic vibrator model.

In all but one of these experiments, excitation probabilities were obtained by measuring γ rays in coincidence with backscattered ions. The quadrupole moment can be obtained by comparing the excitation probabilities which result from using different types of projectiles, keeping the geometry of the experiment fixed. There are two difficulties associated with this type of experiment. First, it is hard to extract from a particle- γ coincidence experiment the excitation probability with the kind of accuracy needed (i.e., 1%). Secondly, it is not possible to differentiate between the effect due to the quadrupole moment of the 2^+ state and possible other higher order effects such as virtual excitation via the giant dipole resonance. Therefore,

it seemed desirable to develop a second and at least partly independent method for measuring quadrupole moments.

In the present experiment the scattered ions are energy analyzed and the quantity measured is the ratio $R_{\text{exp}} = d\sigma_{\text{inel}}/d\sigma_{\text{el}}$ of the inelastic to the elastic cross section as a function of the scattering angle. A similar experiment was performed by de Boer et al.,¹ who measured R_{exp} for different projectiles, keeping the scattering angle fixed.

The experiment was performed with 42-MeV O^{16} ions from the University of Pittsburgh tandem accelerator. The method of production of the oxygen beam is similar to the one employed in other laboratories, with the exception that we use a foil stripper. We typically obtain 0.3 to 1 μA of 6^+ beam on target. The scattered ions are energy analyzed in an Enge split-pole spectrograph and detected by means of position-sensitive detectors.

There are two effects which have discouraged previous attempts to determine excitation probabilities by resolving the inelastic and elastic groups. First, energy losses and straggling are very large, which necessitates the use of